

Appendix A: First-time use, calibration, and testing, of the NW200G balance

This Appendix describes how to do a first-time set-up the NW200G balance, and then how to calibrate and test its operation.

The balance arrives in a single box, together with a 200-g calibration mass, a wall-transformer power supply, and an instructional manual. Identify these objects as you unpack them; then unpack the balance itself. You will also find a stainless-steel weighing pan that needs to be put onto the plastic weighing platform of the balance; learn how to slide open the side doors of the draft cover to access the interior. There is also a flexible plastic ‘splash cover’ that protects the balance’s display and controls from accidental spills; this you should *leave in place* as a permanent part of the balance.

Pick the spot where you will be using the balance – a stable and level table is the main requirement, and freedom from excess draft is another. Now find the bubble level at the left front of the balance, and practice tilting the balance until the bubble is centered in the display. Then use the threaded feet underneath the balance’s base to hold the balance in a level configuration. Ensure that all four, not just three, of these threaded feet are in contact with the table.

Now you are ready to use the balance. Check that you have been supplied a wall transformer that matches your local ac line supply (120 V or 230 V ac). Connect the output cord of the wall-transformer power supply properly to the back of the balance, and then plug the wall transformer into the line. Now find the rocker switch that’s hidden underneath the balance – your right hand’s fingers can find the switch on the undersurface of the balance, along the right edge of its base. When you have flipped that switch, the balance will not yet come on; but it will, once you press the ON/OFF button on its display.

You’ll see the balance go through its boot-up sequence; its display should show 888888, then 203, then V1.1, then 444444, 333333,222222, 11111, and ----- in sequence. It should then settle to a reading of 0.000 g, having automatically assumed the balance pan is empty. If you get none of this display information, or you get an error message, check the balance’s instructions for trouble-shooting.

Now put a light object, such as a jumbo paper-clip, onto the balance’s pan. You should see the display take on a new reading; get accustomed to the timescale over which the reading settles to its final value. That final value should remain stable to ± 0.001 g, but you may need to close both side doors to achieve this stability. Now remove the paper clip, and see the degree to which the display’s reading returns to 0.000 g.

If you are fascinated by the 0.001-g or 1-mg resolution of this balance, try weighing one grain of rice, or one crystal of table salt, or a crystal of table sugar. For familiarization, get a glass microscope slide and weigh it; and then add one fingerprint, as wet and greasy as you like, and weigh it again. This will give you a feeling for what you need (and what you *don’t* need) to worry about in handling samples for weighing.

Calibration

Before you worry about the zero stability, or the calibration, of the balance, you should have let it temperature-equilibrate to its surroundings for a day, and then have it turned on for an hour. Then you can empty the pan, and use the ZERO button to get a 0.000 g indication. Now to perform a calibration, you'll need the 200-g test mass that came with your balance, and nothing else. The calibration procedure will only ensure that the balance will give a reading of 200.000 g when the test mass is on the pan. (It will *not*, for example, test the accuracy of the test mass itself; and it will certainly *not* settle the question of what air-buoyancy corrections or assumptions are being made.)

Here's the calibration procedure:

- Have the 200-g standard mass available, but have it off the weighing pan.
- Use the ON/OFF button to turn the balance OFF, then right back ON. When the boot-up sequence gets to the ----- display, press the ZERO button once.
- The display will change to CAL.; then press the ZERO button once more.
- The display will change to 200.000 with the 2-digit flashing; since this is the mass at which you'll calibrate the balance, you need no changes in this target value. So press the ZERO key once more.
- You'll get a random-looking 6-digit decimal number (it's a numerical representation of a raw analog-to-digital converter output). Wait for that number to settle to ± 1 unit, and then press the UNIT key. The display will show 200.000 with all six digits flashing.
- Only now is it time to place the 200-g calibration mass on the pan. After a few seconds, you'll hear an audible beep, and then you'll get a stable display.
- The balance will have returned to the weighing mode, and should be displaying 200.000 g.
- Remove the calibration mass, and check for a display of 0.000 (± 0.001) g. Restore the 200-g mass to the pan, and check for a display of 200.000 (± 0.001) g.

Calibration is now complete; re-bag and safely store your calibration mass. You might *check* the calibration, using the 200-g mass, each time you use the balance, but it is not clear that you need to *re-do* the calibration each time.

Reality checks for the balance

There are several ways you can test for yourself the degree to which the balance responds correctly to loading by masses.

A **first method** requires borrowing, perhaps from some friendly chemist, a set of calibrated masses, such as a set including 1, 2, 5, 10, 20, 50, and 100-g masses. Your balance, once zeroed and calibrated, has been set to respond correctly at the 0.000-g and 200.000-g readings, but it remains a nontrivial test of its correctness to see what it reads for an object claimed to be of mass 100.000 g.

Another test, of greater relevance to the Gouy method for magnetic susceptibility, is to see how the balance reacts to the addition of a 1-g test mass, first when the pan is empty (so its reading should rise from 0.000 g to 1.000 g) and next when the pan is holding a 100-g mass (so its reading should rise from 100.000 g to 101.000 g).

An **alternative method** of testing the balance requires no access to calibrated masses at all, yet still tests the linearity of its response to mass. For this test, you need only some everyday metal objects, one object of mass near 3 g (think of a penny), and two more objects with masses between 80 and 100 g (think about some bolts or other machined parts). The two ‘heavy’ objects do *not* need to have their masses matched. You can first use the zeroed and calibrated balance to find a mass reading for each of these individually; record the results as m , M_a , and M_b respectively.

Now put the light object, and the a -object, both on the pan. You know the balance’s reading ought to be $m + M_a$; but is it, in fact? Similarly, you can use the light object, and the b -object, both in the pan; do you in fact get the expected result $m + M_b$?

Finally, you can record the readings you get, in succession, for the empty pan, for the a -object; for the b -object, and finally for the a - and b -objects loading the pan together. For the last of these cases, do you in fact get the reading you expect, namely $M_a + M_b$?

You might know the terminology for what you’ve done: you’ve checked the ‘differential linearity’ and the ‘integral linearity’ of the balance’s response to loading. In making measurements of magnetic susceptibility, you’ll care most about differential linearity, since you’ll be looking for small departures (of size 0.01 g to a few grams) from a large ‘dead weight’ reading of the magnet structure’s mass. You should therefore get familiar with the accuracy, and the time-scale for settling, of the balance to this sort of small changes in its load.

Turning the NW200G into a Gouy balance

When you have familiarized yourself with the operation of the balance, you are ready to convert it to a Gouy balance. To do so, follow the procedure laid out in Section 3(b) of the Manual, “Setting up the apparatus”.

Appendix B: The standard samples provided by TeachSpin

This Appendix describes the sixteen filled sample tubes that are ‘standard samples’ provided with your Foundational Magnetic Susceptibility set-up. You are, of course, encouraged to use the 24 extra empty sample tubes that come with your kit to investigate other samples; the procedure for filling such tubes is found in Appendix C. But here are comments on the already-filled tubes.

Empty sample tubes, without their covers, have a mass near 2.62 g – you can measure several ‘empties’ to learn how reproducible this number is. Thus you can measure the mass of a filled as-supplied sample tube, again without its cover, to deduce the mass of the sample that’s contained in it. (This is a simpler procedure than emptying out the sample for weighing.)

TeachSpin-filled sample tubes are assigned a number (from 1 through 16) and have that number, and an abbreviation, hand-written onto the (frosted-finish) side of the tube. We use ‘permanent marker’ pens, and we have confirmed that the ink is not measurably magnetic. Here are the details of the samples:

#1-3 are solid bar samples of metal, nominally 3/8" square; you can measure their actual dimensions for yourself.

- #1. This bar is copper, of 110-alloy composition, nominally 99.9% copper.
- #2. This bar is aluminum, of 1100-alloy composition, >99% aluminum (and <0.7% combined Si and Fe).
- #3. This bar is titanium, of Grade-2 composition, >99.2% titanium.
- #4. This is bismuth, in pellet (ie. shot) form, and >99.9% bismuth in composition.
- #5. This contains a piece of cobalt wire, of 99.99% purity, of 5-mil = 0.005" = 127 μm diameter. The wire, of length 32 mm, is held by a paper ‘Z-fold’ to stand vertically in the center of the cuvette. There is no reason to suppose that it acts like a paramagnetic material with constant χ ; yet it certainly gives a magnetic ‘signal’ in a Gouy balance.
- #6. This contains two slabs of pyrolytic graphite, each of width 7.5 mm, height 32 mm, and nominal thickness $\frac{3}{4}$ mm. The two slabs are held against the frosted sidewalls of the cuvette by a paper Σ -fold.
- #7. This contains (coarsely-crystalline, variable-color [try viewing it under skylight, incandescent, and fluorescent light!]) neodymium chloride hexahydrate, $\text{NdCl}_3 \cdot 6\text{H}_2\text{O}$, of >99.9% purity. (This material replaces the Nd_2O_3 formerly used, which was subject to water-vapor absorption and swelling.)
- #8. This contains (off-white, finely-powdered) gadolinium oxide, Gd_2O_3 , of >99.9% purity.

- #9. This contains (strawberry pink, finely-powdered) erbium oxide, Er_2O_3 , of >99.9% purity.
- #10. This contains (pale blue, coarsely-powdered) ‘Mohr’s salt’, ferrous ammonium sulfate, or ammonium iron(II) sulfate hexahydrate, $(\text{NH}_4)_2\text{Fe}(\text{SO}_4)_2 \cdot 6\text{H}_2\text{O}$.
- #11. This contains (pale-purple-yellow, coarsely-powdered) ‘iron alum’, ferric ammonium sulfate, or ammonium iron (III) sulfate dodecahydrate, $\text{NH}_4\text{Fe}(\text{SO}_4)_2 \cdot 12\text{H}_2\text{O}$.
- #12. This contains (blue, coarsely-powdered) ‘blue vitriol’, copper(II) sulfate pentahydrate, $\text{CuSO}_4 \cdot 5\text{H}_2\text{O}$.
- #13. This contains (turquoise) copper acetate, sometimes called monohydrate and written as $\text{Cu}(\text{OAc})_2 \cdot \text{H}_2\text{O}$ where OAc is chemists’ lingo for acetate. The molecules are actually dimers, and the structure is $[\text{Cu}(\text{CH}_3\text{COO})_2 \cdot \text{H}_2\text{O}]_2$ or $\text{Cu}_2(\text{CH}_3\text{COO})_4 \cdot 2\text{H}_2\text{O}$, which is accordingly also called dihydrate.
- #14. This contains (green) manganese oxide, MnO .
- #15. This contains (pale pink) manganese chloride tetrahydrate, $\text{MnCl}_2 \cdot 4\text{H}_2\text{O}$.
- #16. This cuvette contains, as its active ingredient, a fine powder of nickel-zinc ferrite, written as $\text{Ni}_x\text{Zn}_{1-x}\text{O} \cdot \text{Fe}_2\text{O}_3$. So the $x=1$ limiting case would be the mixed oxide $\text{NiO} \cdot \text{Fe}_2\text{O}_3$, nickel ferrite, sometimes written as NiFe_2O_4 . The ferrite is an electrically-insulating ferromagnetic material, and it might not be characterized by a constant χ . To keep its Gouy-method signals within bounds, some ferrite powder has been dispersed among a much greater fraction of powdered alumina, Al_2O_3 . That mixed powder is in turn mixed with powdered wax, and the ferrite/alumina/wax mixture is finally warmed to lightly sinter the mixture together (to keep the denser ferrite powder uniformly spread throughout the sample, rather than settling to the bottom of the cuvette with time). The proportions-by-mass of the mixture from which the cuvette was filled are 0.55% of ferrite, 64.91% of alumina, and 34.54% of powdered wax.

Notice: While none of these 16 materials is notoriously poisonous, it does *not* follow that they are automatically harmless! Some of them are known to be toxic, to some organisms, at some concentrations. Some of them are water-soluble. The finely-powdered materials can spread in air if spilled. So in general, keep these materials covered, either by their caps, or by the cap at the bottom of the lifter rod when the samples are in use. And make it a professional safety habit to look up the properties of any material you have occasion to use, or to talk with someone more experienced in its use than yourself.

Appendix C: Sample Preparation

The TeachSpin method for measuring magnetic susceptibility allow you to prepare samples of your own choice of materials, and measure them by the Gouy method.

In the TeachSpin version of the Gouy technique, all you need do for sample preparation is to fill a plastic cuvette (of internal dimensions 10.0 mm square) to a measured height, and to fill that height uniformly with your target material. You will also want to weigh, to 0.01-g resolution, the empty and capless cuvette, and then weigh it again after filling, to infer the mass of the sample you've added.

There are very few issues with loading a *liquid* sample, except that you don't want to use a solvent that dissolves the plastic! (The cuvette material is polystyrene, which in its more familiar foamed form is called Styrofoam. Such plastic is impervious to water, but is notoriously soluble in acetone and some other organic solvents.) When loading a powdered *solid* sample, you may have difficulties on getting the powder to give a uniform filling of the volume inside the cuvette. Standard fixes are gently tapping the bottom of the cuvette on a tabletop during the filling process, and/or the use of a plastic 'tamper' to compress a powder into a smaller volume.

Certain powders are subject to irregular packing, especially if you postpone tamping until the end of the process. The goal is *not* to achieve a 100% filling fraction of the volume inside the cuvette, but rather to achieve a uniform filling. Knowing the mass of the sample added, and the height to which it fills the cuvette, is sufficient for giving you the mass susceptibility of the sample, *whether or not* you know the filling fraction or the density of the sample.

Any sample worth making and measuring is certainly worth documenting and capping for future use. One technique is to write the essential information on a Post-It note to be affixed to the cuvette, and to keep that label on the cuvette at all times (except in its actual use in weighing). You might also assign a sample number, and record essential information in a log book. A metal stylus can be used to scratch a permanent sample-number onto the plastic wall of the cuvette, or a 'permanent marker' will write onto the frosted exterior surface of the cuvette.

Finally, you should be aware of 'chemical hygiene'. No one will fault you for filling sample cuvettes with table salt, sugar, water, baking soda, or other materials 'generally recognized as safe'. But if you are using any chemical sample you'd rather not have served you on a plate or in a cup, you owe it (to yourself, your peers, and your institution) to observe all the safety requirements appropriate to the materials you're using. If you are uncertain of the safety of any sample you choose to prepare, get information *first*, before you even procure your material. Just because you temporarily care only about a sample's magnetic properties does not mean that the possible hazards of its chemical or biological reactivity have ceased to act!

Appendix D: Magnetic surveying and linearity of magnetization

This Appendix teaches how to use one accessory to the Foundational Magnetic Susceptibility apparatus, a tool which puts vertical translations of the lifter structure onto a calibrated scale of motion. With this ‘surveying’ tool, there are new measurements that can be made. In particular, this appendix offers the optional exercise of testing if the magnetization M really is, or is not, a linear function of the magnetic field H . In cases where linearity is confirmed, the method only reproduces the same results for the coefficient of proportionality, χ , that the Gouy method has already established. But even in that case, it can make possible a susceptibility measurement that requires a much smaller volume or mass of sample material.

The other advantage of this optional technique is that it tests, very directly, the ‘differential’ form of the predicted vertical force derived earlier,

$$\Delta F_z = +\mu_0 \chi H_y \frac{\partial H_y}{\partial z} \Delta V .$$

In particular, confirmation of this result shows that the force on a sample of dia- or paramagnetic material is *not* proportional just to the magnetic field, nor just to its gradient, but to the product of the two factors. You are free to imagine that a field H creates in a volume ΔV of sample a magnetic moment $\mu = M \Delta V = \chi H \Delta V$, and that the field’s *gradient* is then the agent responsible for exerting a force on this newly-created magnetic moment. And, by conducting this test in varying values of the field, and looking to see if vertical forces scale according to the above equation, this optional method tests to see if χ really is a field-independent constant. In particular, this is a test that saturable ferromagnetic materials are expected to *fail*.

There are almost no new tools required for this new ‘surveying’ method; in particular, it uses the same current-hairpin as a method for measuring magnetic field, and the same sample holders for testing the action of this field on samples. The only new tool required is a simple structure that makes possible a quantitative measure of the vertical translations of the current-loop and sample-holder – it’s the ‘lifter elevator screw’ that came with your FMS equipment.

That tool, found in a bag labelled SUB-FMS01-13, is to be installed into the brass part of the lifter structure as shown in the photo below. When the threaded rod reaches the bottom of the threaded hole in the brass, finger-tighten the small nut down onto the brass to lock the threaded rod against rotation. Now the thumbscrew will constrain the vertical position of the sample-holder. The value of this technique is that the thumbscrew will move vertically, by just the pitch of the threaded rod, for every full rotation of the thumbscrew. The threaded rod you are using has a pitch of 40 turns per inch, so one full turn of the thumbscrew moves the vertical constraint by $25.4 \text{ mm}/40 = 0.635 \text{ mm}$. Note the dark marker-spot on the top of the thumbscrew, and note that it can be easily set, to considerable precision, to positions just 360° apart after one rotation. Each such full turn will give you a translation of $\Delta z = 0.635 \text{ mm}$. You will need to keep count of the number of turns you have moved the nut from some reference position.

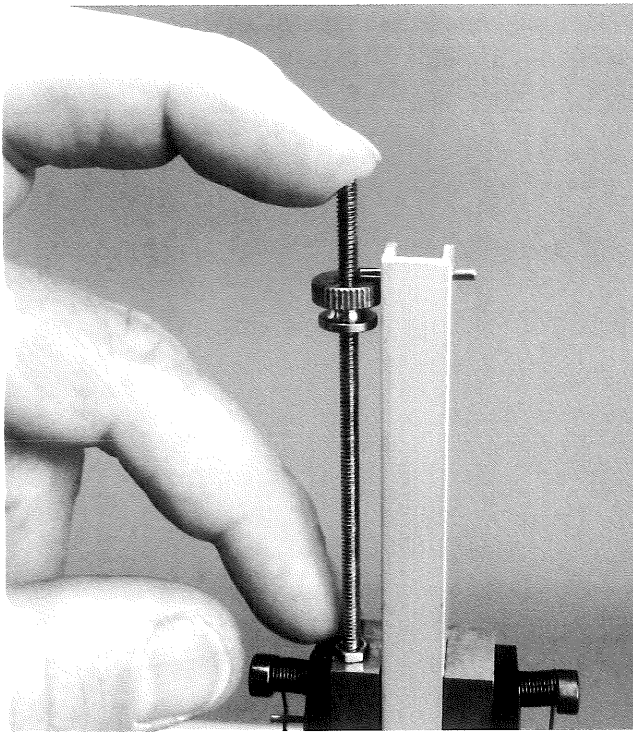


Fig. D.1: The translation-in- z structure, installed and in use

Magnetic field surveying

This section has nothing to do with dia- or para-magnetism, and everything to do with surveying the vertical variation of the magnetic field \mathbf{B} produced by the permanent-magnet structure. We will again adopt the coordinate system in which the field \mathbf{B} is largely in the horizontal y -direction, the bottom of the current-hairpin carries current i in the horizontal x -direction, and the magnetic interaction between the field and the current produces a vertical force ΔF_z which is rather directly sensed by the balance. Once again we will neglect the forces exerted on the vertical side-walls of the current-hairpin structure, and here we will neglect the variation of the field over the area, about 1 cm^2 , of the bottom of the hairpin. Then the previous result,

$$\Delta m = \frac{1}{g} \Delta F_z = \frac{i L_x B_y}{g} ,$$

shows that we can measure the field B_y , averaged over the 1-cm^2 area occupied by the bottom of the hairpin, even if that cm^2 of conductor is not in the ‘sweet spot’ at the center of the permanent-magnet structure where the field is largest.

So let the new translation structure establish for you a vertical z -scale; now by locating the current-hairpin at varying values of z , and measuring the response Δm to current i as a function of the z -coordinate, you can establish the variation of B_y as a function of z . You will need to ‘survey’ for perhaps 30 mm to either side of the (experimentally-determined) location where B_y reaches its maximum value. You will need to take enough points to follow the variation of $B_y(z)$, using a sufficient density of points on the ‘shoulders’ of the curve you will obtain. The plotted

data will show you what is the right place to label as $z=0$; you should note that this is expected to occur when the bottom of the current hairpin is centered vertically in the magnet structure, as confirmed by viewing through the magnet's sighting holes. Previously, this was the only place you needed to make a field measurement, and you didn't need to know where in z it occurred, since you merely found the place giving an extremum in ΔF_z .

[When the bottom end of the current hairpin is sampling the B -field well *below* centerline of the magnet structure, you will find curious results from the current-hairpin survey. One reason will become clear when you look at the wiring of the *top* end of that current hairpin, and note its position relative to the magnet. Implication: your current hairpin is really only suited to surveying the 'top half' of the field profile; you can estimate the field profile's 'lower half' by assuming reflection symmetry with its upper half.]

The 'peak value' of this $B_y(z)$ curve should match the single B_y -value that you previously used in calibrating the Gouy method, but now you will have more information. You will *not* have a curve which is easily compared to theory, however. The theoretical modeling for the curve you have obtained empirically would require a quite elaborate exercise in finite-element magnetostatics. Even if you were to ignore the effects of the steel return-flux yoke of the magnet, and to model each of the two permanent magnets as thin circular current loops, you'd still have a formidable 3-d problem computing the field due to circular coils, but at test points *not* on the axis of cylindrical symmetry. All you can say on theoretical grounds is that for small z -values, the field is nearly constant at some value B_{\max} , while at large z -values, the field ought to drop off as z^{-3} ; so a very naïve model for the field would be

$$B_y(z) \approx B_{\max} \frac{a^3}{(a^2+z^2)^{3/2}} .$$

This is a two-parameter model, and you can try best-fitting the values of the peak field B_{\max} and the scale parameter a to see if it does at all well in matching your survey data. The 'fit' might not be good enough for the uses to which you will put the empirical data, however! In fact, you'll see that what you really want is a plot, and/or a model, for $[B_y(z)]^2$. Go ahead and make this plot, and overlay it with a two-parameter model for $[B_y(z)]^2$, to see the successes (and the deficiencies) of this modeling.

Magnetic-interaction surveying

Now that you've surveyed the field $B_y(z)$, it is time to remove the current-hairpin structure, and insert the usual sample-tube holder structure in its place. For a first exercise, we suggest that you prepare a sample tube with a rather small amount (perhaps 1-2 mm in vertical extent) of a rather strongly paramagnetic material (so that signals will not be too small). You will be preparing an approximation to a 'point sample', which can be assigned a single z -value as a location, and which has only a 'differential' volume ΔV . Then you will be translating that sample vertically, using the same calibrated-in- z translations you have used before. Once again, you will infer from the data itself the right place for assigning a $z=0$ value.

In preparing your sample tube, you will want to weigh the empty and capless tube before, and again after, adding your chosen sample material, to learn the mass of the sample you are using. And you may want to build a flat-ended tool of about $(9\text{ mm})^2$ cross section as a ‘tamper’, used temporarily in packing your sample into the tube to create a flat upper surface, just as the bottom of the sample tube creates its flat lower surface.

Now at a variety of choices for the z -position of the sample, note the apparent mass of the magnet. Subtracting the ‘dead weight’ of the magnet, you will get a value of the magnetically-created apparent mass change Δm for each z -value you use. Make a plot of the function $\Delta m(z)$ that you find, and confirm immediately that it looks entirely *unlike* the field profile $B_y(z)$, and also entirely *unlike* the field-squared profile $[B_y(z)]^2$, that you have obtained from your previous surveying.

In fact, those B -field-surveys are very nearly even (symmetric under $z \leftrightarrow -z$) functions of z , while the magnetic-interaction signal $\Delta m(z)$ is very nearly an odd (antisymmetric under $z \leftrightarrow -z$) function of z . This is direct proof that the magnetic forces you’ve been detecting are not directly proportional to B , nor to B^2 . Instead, those forces are proportional *jointly* to field and to gradient, or alternatively, are proportional to the gradient of field-squared. You can show that the expected $\Delta m(z)$ signal should be given by

$$\Delta m(z) = \frac{\Delta F_z}{g} \cong \frac{\chi \Delta V}{2\mu_0 g} \cdot \frac{\partial}{\partial z} [B_y(z)]^2 ,$$

so it’s not the value, but instead the z -derivative, of your previously-drawn $[B_y(z)]^2$ curve that should mimic the $\Delta m(z)$ curve you have taken using your sample.

To make this comparison quantitative, you’ll need the volume ΔV , which is hard to estimate with a powdered sample. Ignoring the susceptibility of the air between the grains of powder, and using m_1 for the mass of sample present, and ρ_1 for its density (in solid form), you can show the above equation can be written as

$$\Delta m(z) \cong \left(\frac{\chi_1}{\rho_1}\right) \frac{m_1}{2\mu_0 g} \cdot \frac{\partial}{\partial z} [B_y(z)]^2 ,$$

and once again the *mass* susceptibility χ/ρ of your material #1, the stuff of the powder, has emerged. Everything else in this equation is already determined, except for the challenge of getting an estimate for the shape and the values of the z -derivative of a function $[B_y(z)]^2$ that you have obtained only by a point survey. If you’ve surmounted that challenge, and if you can find a single value of χ/ρ that makes the two (independently-measured!) sides of this equation agree, then you have shown that χ/ρ really is a field-independent quantity.

And is this a real test? Sure it is – it would *fail* for generic paramagnets at sufficiently high field B , or better still for sufficiently high values of the quotient $\mu_B B/(k_B T)$, since in that limit the magnetic moment *saturates* rather than continuing to grow with B . And it will also fail for those ferromagnetic materials in which saturation occurs even under room-temperature conditions. You could, for example, conduct an experimental test of the latter prediction by making a ‘point sample’ from a tiny chip of commercial ferrite (<20 mg will suffice) glued to the bottom of a sample tube, or making a sample of small vertical extent out of thin nickel foil, cut and stuck into

the bottom of a sample tube. Samples like this might be expected to show a very large value of susceptibility at small value of the B -field, but a χ -value which seems to *drop* in higher-field regions, where large B creates saturation, rather than increasingly large values of magnetic moment.

Now, what is the *use* of this technique? There is the saturation test mentioned above, and the satisfaction of confirming the gradient-modelling you have done. But if you are sample-quantity-limited, ie. if you have only the limited quantity of sample that your research project provides, you might not *have* enough material to fill a usual height of 30-34 mm of sample tube to execute the Gouy type of measurement. Then this ‘point-sample’ sort of measurement may be the only measurement you can make. And from this kind of measurement you can still get accurate measurements of susceptibility, either by using the equation above with a modelled-from-survey field-squared profile, or (alternatively) by comparison of your ‘unknown’ point-sample with another point-sample made using another material which is *not* in short supply, a material whose susceptibility you have previously measured using the Gouy technique.

[Alternatively, you can plot $\Delta m(z)$ data as obtained above, and *integrate* that plot with respect to z from (say) z_1 to z_2 to get a result depending not on the field profile, but only on the difference $B_y^2(z_2) - B_y^2(z_1)$. Assuming the fields at those two points can be measured accurately, and assuming also that the sample has magnetization linear in H , then this method can give the mass susceptibility χ/ρ directly. The technique is called the Thorpe-Senftle method, and it requires more measurement effort, but less sample material, than the Gouy method.]

More modelling in the Gouy geometry

Once you have a magnetic survey giving you the field profile $B_y(z)$, you have the information which will illuminate how the Gouy method works *elsewhere* than those ‘high’ and ‘low’ positions of the sample which give the maximal changes in the apparent mass of the magnet. Recall that in the Gouy method, you use a sample, assumed to be uniformly distributed over a vertical height of h , translated vertically between two special positions. The ‘high’ position of the sample puts the top end of the sample in a weak field, and the bottom end of it at the magnet’s center, in the maximal field B_{max} . Conversely, the ‘low’ position puts the top of the sample in field B_{max} , and the bottom of it a weak field. This gives the two extreme values of the apparent mass change

$$\Delta m = \frac{\chi A}{2\mu_0 g} (B_{top}^2 - B_{bottom}^2) \rightarrow \frac{\chi A}{2\mu_0 g} (0^2 - B_{max}^2) \text{ or } \frac{\chi A}{2\mu_0 g} (B_{max}^2 - 0^2).$$

Because these two positions revealed themselves by causing extrema in apparent mass changes, you did not need to know where in z they occurred. But now you can continuously vary the coordinate z which locates (say) the bottom of the sample, and with it, the coordinate $z + h$ which locates the top of the sample. Then the predicted mass-change takes the predicted form

$$\Delta m = \Delta m(z) = \frac{\chi A}{2\mu_0 g} ([B_y(z + h)]^2 - [B_y(z)]^2) .$$

This is not a function that’s easy to visualize, but it is easy to plot, if you have even an approximate analytical model for the function $B_y(z)$. When you plot such this Δm function, you should see emerging the two extreme values of Δm which you have previously used for data reduction in the Gouy method. But you should also see, as a function of z , all the intermediate values of $\Delta m(z)$ as well. These values will include a spot value of $\Delta m = 0$, obtained when the sample’s bottom is at $z = -h/2$; this corresponds to locating the sample in the z -range $-h/2$ to $+h/2$, ie. the sample is vertically-centered in the magnet. The use of this new prediction is that you could now take Gouy Δm data not just at the two extremal- Δm values you previously used as the ‘high’ and ‘low’ positions, but over a whole range of z -values. The option is to see whether the balance’s readings of Δm reproduce the model’s predictions of Δm , both as functions of z .

To get those predictions to match will require a decent model, either empirical or best-fit, of the function $B_y(z)$. It will also require numerical values for the parameter χ , the volume susceptibility of the sample – for a powdered sample, this would be a volume-weighted average of the susceptibilities of the material of interest, and the air between its grains. Finally, a match between predicted and observed models for $\Delta m(z)$ will require a sample that is uniform along its vertical dimension, and one which really is characterized by a constant χ . So if the material is ferromagnetic but subject to saturation, you might detect such magnetic saturation via a mismatch between prediction and observation.

Perhaps the best pair of samples to use in such an investigation are the rare-earth oxides (which gives large signals from paramagnetism, but is unlikely to be saturating magnetically) and the cobalt-wire or ferrite-containing samples (which also gives large signals, but arising from ferromagnetism, and hence subject to saturation).

Appendix E: Non-ideal features of the permanent-magnet's field

This TeachSpin apparatus for measuring magnetic susceptibility uses the Gouy technique, which requires access to a convenient magnetic field: one that's large, constant, and uniform in one place (say at the bottom end of a sample, or of a current hairpin), but which is negligibly small at another place (say at the top end of a sample). If you've done the measurements and the calibrations of Ch. 3, you've seen that this magnet can have its field calibrated from first principles, and that it then give values of magnetic susceptibility for samples. But now this Appendix takes up the harder question: how does the *actual* magnetic field you've used differ from the ideal field you've assumed? And what systematic errors does this difference create?

The ideal case

We adopt a coordinate system in which the z -axis is vertical, and the permanent magnet's B -field is chiefly horizontal and along the y -direction. So the y -axis can be taken to pass through the centers of the two circular faces of the permanent magnets, and we can take the origin of an xyz -coordinate system to lie in the geometrical center of the magnet-structure's air gap. In this picture of the ideal magnet, the magnetic field is taken to be $\mathbf{B}(\mathbf{r}) = B_0 \hat{\mathbf{y}}$ over the full volume of that air gap, but is treated as negligible outside of that air gap.

In this model, the current hairpin, when suitably aligned, has its bottom segment defines a vector which is of magnitude L and wholly directed along the x -axis. When it carries current I , it creates a force (of the magnet, on the current) of $\mathbf{F}_{\text{mag}} = IL \times \mathbf{B} = IL \hat{\mathbf{x}} \times B_0 \hat{\mathbf{y}} = (IL B_0) \hat{\mathbf{z}}$. A force of the same magnitude, opposite in direction but still vertical, describes the force of the current-hairpin on the magnet. That's the force which the balance displays as an apparent mass change Δm , where

$$\Delta m \cdot g = F_z = IL B_0 .$$

The value $(\Delta m \cdot g)/(IL)$ then gives B_0 , the desired value of the magnetic field within the magnet's air-gap volume.

Now the use of a magnetic-susceptibility sample (say in the 'high' position) has the top end of a sample in a $B \approx 0$ region, while the bottom end lies in $\mathbf{B} = B_0 \hat{\mathbf{y}}$. We've seen that a (vertically-uniform) sample of cross-sectional area A then experiences a vertical force

$$\Delta F = \frac{\chi A}{2 \mu_0} (B_{\text{top}}^2 - B_{\text{bottom}}^2) ,$$

and this shows up as another apparent mass change on the balance, of

$$\Delta m = \frac{\Delta F}{g} \cong \frac{\chi A}{2 \mu_0 g} (0 - B_{\text{bottom}}^2) .$$

There's a useful interpretation of this ΔF , coming from the 'virtual work' concept. For the sample tube to be raised by height increment $\delta z = 1$ mm, a work increment of $\delta W = \Delta F \delta z$ would be required, and this would be equal to the change in energy of the magnet-plus-sample system.

To understand that energy change in another way, note that in this procedure each horizontal slab of sample would rise by 1 mm. For a uniform sample, that would make no difference anywhere along the sample (as one slab of material in space would be replaced by another, identical, slab of material), *except* that there'd be less volume (by $1 \text{ mm} \times A$) of sample in the high-field region, and more volume (also $1 \text{ mm} \times A$) of sample in the $B \approx 0$ region. So the cost in magnetic energy of lifting the whole sample by $\delta z = 1 \text{ mm}$ can be understood as the cost, in magnetic energy, of moving only the bottom slab (of volume $1 \text{ mm} \times A$) from the bottom, to the top, of the sample region. It follows that we care about the field values B_{top} and B_{bottom} only – not about any details of the field between these two planes.

The non-idealities of the actual field

The actual magnetic field is more complicated than the ideal one in several ways; it is not uniform in magnitude or direction, even over the ($10 \text{ mm} \times 10 \text{ mm}$) area of the bottom of the sample, and it is certainly not uniform over the whole volume of the current-hairpin or the sample.

Let's look first at the case of the current hairpin, the force on which is $\Sigma (i \, dl \times B)$. Here the i s are local current elements, sub-parts of the net current I , and the dl s give the vector directions of these currents, and the sum is taken over *all* the parts of the current hairpin. Meanwhile, B has a local value, certainly very different from $B_0 \hat{y}$ on some parts of the hairpin's side segments. How does this matter? We are materially aided by the fact that balances are designed to register only *vertical* forces; here these are given by

$$(F)_z = \Sigma (i \, dl \times B)_z = \Sigma i (dl_x B_y - dl_y B_x) .$$

Because of the absence of terms in dl_z , we see that currents in the vertical segments of the hairpin (where we can assume currents are in the $\pm z$ -direction) create no forces that the balance will register. That leaves only the ‘bottom’ of the hairpin to develop forces that matter. Next, we note that over the area of the bottom of the hairpin, we can assume current flow almost purely in the x -direction, so the dl s have $dl_y \ll dl_x$, and we note further that in this region, any B_x s have $B_x \ll B_y$. Thus the second term in the sum above is made of products that are ‘doubly small’ relative to the first term, and hence we'll neglect them. What remains is

$$(F)_z = \Sigma (i \, dl \times B)_z = \Sigma i (dl_x B_y) .$$

If B_y were to be uniform, and of magnitude B_0 , over the whole bottom of the hairpin, this sum would reduce to $I L B_0$ as previously assumed. But the worry is that B will differ, in magnitude and direction, from this uniform-field model. So we need to deal with the sum shown, but summed over the full region $-5 \text{ mm} < x < +5 \text{ mm}$, $-5 \text{ mm} < y < +5 \text{ mm}$, and $z = 0$, when B is *not* uniform.

Similarly in measuring the susceptibility χ : we need the value of the field B^2 , averaged over this area of ($10 \text{ mm} \times 10 \text{ mm}$) at the bottom of the sample, in the $z = 0$ plane. The average of B^2 , written as $\langle B^2 \rangle$, will have value B_0^2 only if the field is spatially uniform. But it's not!

Looking down at the magnet from above, here's a qualitative sketch of how the field lines of \mathbf{B} must look, in the $z = 0$ xy -plane:

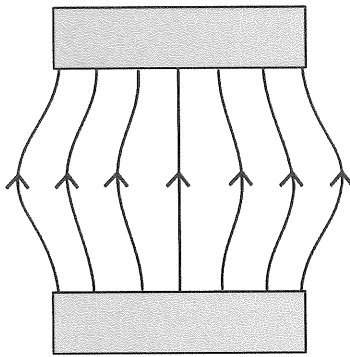


Fig. E.1: a sketch of B -field lines in the $z=0$ xy -plane

The field lines ‘bulge’ as sketched, and this tells us the field is stronger near the pole faces than in the middle, where $y = 0$ along the x -axis. That is to say, $|\mathbf{B}|$ grows as y departs (either way) from $y = 0$; similarly, we expect $|\mathbf{B}|$ to shrink as x departs (either way) from $x = 0$.

Another sketch of the field, from the same viewpoint, shows not the field lines, but instead the field *vectors* and their components:

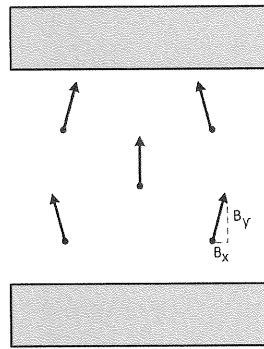


Fig. E.2: a sketch of B -field vectors in the $z=0$ xy -plane

This shows us that B_y is an even function of y , and also an even function of x , assuming left-right and up-down symmetry in the diagram. But we also see an antisymmetry, which tells us that B_x is an odd function of y , and also an odd function of x . We also see that at general locations, \mathbf{B} has both x - and y -components; for example, in the first quadrant of the xy -plane, we see a vector telling us that $B_x < 0$ while $B_y > 0$.

The lowest-order Taylor expansion of field components, around the $x = 0 = y$ point, having all these properties is

$$B_y(x, y) = B_0 - \alpha x^2 + \beta y^2 + \dots, \quad B_x(x, y) = 0 - \gamma x y \dots$$

where we've written all the terms that can appear through second order in small quantities. In the form in which we've written the expansion, and given the sketches above, we expect the constants α, β, γ that appear will all be *positive* in value.

But these three constants are not independent, since Maxwell's Equations require $\nabla \cdot \mathbf{B} = 0$ everywhere, and $\nabla \times \mathbf{B} = 0$ everywhere in the air gap. In our case, these equations give

$$\frac{\partial B_x}{\partial x} + \frac{\partial B_y}{\partial y} = 0 ; \quad \frac{\partial B_x}{\partial y} - \frac{\partial B_y}{\partial x} = 0 ,$$

which translate into

$$(-\gamma y) + (0 + 2\beta y) = 0 ; \quad (-\gamma x) - (0 - 2\alpha x) = 0 .$$

For these to be true in the entire neighborhood of the origin, we require $2\beta = +\gamma$, and $2\alpha = +\gamma$. Hence the whole field model can be summarized in terms of *one* positive constant γ as

$$B_y(x, y) = B_0 + \frac{\gamma}{2}(y^2 - x^2) + \dots , \quad B_x(x, y) = -\gamma x y \dots$$

It would require some very complicated modelling of the circular pole-faces, and the outer steel yoke, of the permanent-magnet structure to make a theoretical prediction for the value of γ , the sole non-ideality parameter that remains. We seek here, instead, to *measure* γ empirically (using the current hairpin!), and then to see its consequences for the use of the Gouy method.

Measuring the actual magnet's non-ideality

We assume a field model, described in the $z = 0$ plane and for small x - and y -values, as given by the equations above, and now we imagine a current hairpin whose bottom surface is a square, 10 mm \times 10 mm, carrying net current I in the x -direction. So the relevant area of (horizontally-directed) current is a square of side $2a = 10$ mm. But now we imagine that the square is properly centered in the $z = 0$ plane, and centered about the $y = 0$ point, but is deliberately displaced 'sideways' by amount δ along the x -axis. Thus the current-hairpin's bottom lies in region

$$-a + \delta < x < +a + \delta , \quad -a < y < +a , \quad z = 0 .$$

This 'translation sideways' is easily accomplished in actual experiment, by using a sliding degree of freedom of the lifter structure relative to the balance cover on which it sits. The idea is to measure the force F_z arising from current I in the hairpin, as a function of this displacement δ , and to use this information to tell us the value of the field-inhomogeneity parameter γ .

So we use $F_z = \Sigma (i dl \times \mathbf{B})_z$, and we divide the net current I into infinitesimal current elements. A stripe of width dy carries current $di = (I/(2a)) dy$, flowing (we assume) in the x -direction, so $dl = \hat{x} dx$. Then

$$F_z = \Sigma (i dl_x B_y) \rightarrow \iint_A \frac{I dy}{2a} dx B_y(x, y) = \int_{-a+\delta}^{a+\delta} dx \int_{-a}^a dy \frac{I}{2a} \left[B_0 + \frac{\gamma}{2}(y^2 - x^2) \right] .$$

The result of the double integration is

$$F_z = I(2a)B_0 + I \frac{\gamma}{2} (-2a \delta^2) .$$

So using L for the length of the hairpin's bottom, $2a$, we can write

$$F_z = ILB_0 \left[1 - \frac{\gamma \delta^2}{2 B_0} \right].$$

Notice that the result for $F_z(\delta)$ reduces exactly to the previous value of ILB_0 for $\delta = 0$, despite the inhomogeneity of the field. So the method of Ch. 3 for calibrating B_0 is not wrong, and needs no correction, despite the imperfections in the field. But we have also shown that $F_z(\delta)$ does indeed drop below its maximum, upon translation of the hairpin along the x -direction. If we were to find that it drops by 1% for a translation by $\delta = \pm 2$ mm, we'd have shown that

$$1 - \frac{\gamma (2 \text{ mm})^2}{2 B_0} = 0.99, \text{ or } 0.01 = \frac{\gamma (2 \text{ mm})^2}{2 B_0}, \text{ so } \gamma = 0.005 \frac{B_0}{(\text{mm})^2}.$$

In practice, to determine B_0 and γ one would want to take $F_z(\delta)$ data over a range of δ -values, and look for a region about $\delta = 0$ that's successfully fit by a quadratic model, and fit the data in that region by a model $F_z(\delta) = c_0 + c_2 \delta^2$, to get best estimates for the parameters.

Note that this γ -value emerges from current-hairpin data alone, without any reference to magnetic susceptibility. The value of γ depends on empirical data, reduced using a plausible model of the field inhomogeneity derived by reference to Maxwell's Equations.

Consequences, for susceptibility measurements, of the non-ideal field

So now we assume the *non-ideal* field model, described by parameters B_0 and γ that are determined by current-hairpin measurements. We want to know how the vertical force we measure using such a magnet in the Gouy technique will *differ* from what we've computed for the ideal field.

To do so, we assume that the force in question is connected to the magnetic energy of the bottom-most slab of the sample, and that we've properly located this slab in the $z = 0$ midplane of the magnetic field. We then expect

$$F_z = \frac{\chi A}{2\mu_0} (-\langle B^2 \rangle),$$

where we need the average-of- B^2 over the region $-a < x < a$, $-a < y < a$, and $z = 0$. That is to say, we locate that bottom-slab-of-sample properly, putting it into place centered about $x = 0 = y$. But since the B -field is not uniform over that area, we expect that the average-of- B^2 will differ from the value B_0^2 that pertains to the center of that area.

Given our field model, in the $z = 0$ plane we have $B^2 = B_x^2 + B_y^2$, where

$$B_x^2 = +\gamma^2 x^2 y^2; \quad B_y^2 = B_0^2 + 2 B_0 \frac{\gamma}{2} (y^2 - x^2) + (\frac{\gamma}{2})^2 (y^2 - x^2)^2,$$

so upon combining terms and simplifying we get

$$B^2 = B_0^2 + \gamma B_0 (y^2 - x^2) + \frac{\gamma^2}{4} (y^4 + 2y^2x^2 + x^4).$$

Now using $\langle \rangle$ to indicate averages taken over our square,

$$\langle f(x, y) \rangle \equiv \frac{1}{(2a)^2} \int_{-a}^a dx \int_{-a}^a dy f(x, y),$$

we see the need for the easily-done integrals

$$\langle y^2 \rangle = \frac{1}{3} a^2, \quad \langle x^2 \rangle = \frac{1}{3} a^2, \quad \langle y^4 \rangle = \frac{1}{5} a^4, \quad \langle y^2 x^2 \rangle = \frac{1}{9} a^4, \quad \langle x^4 \rangle = \frac{1}{5} a^4.$$

Thus we finally get for the average-of- B^2 as

$$\langle B^2 \rangle = B_0^2 + \gamma B_0 \left(\frac{a^2}{3} - \frac{a^2}{3} \right) + \frac{\gamma^2}{4} \left(\frac{1}{5} + \frac{2}{9} + \frac{1}{5} \right) a^4 = B_0^2 + 0 + \frac{7}{45} \gamma^2 a^4.$$

Sure enough, the value of $\langle B^2 \rangle$ we get really is bigger than B_0^2 (though the correction term that emerges is of order γ^2 , not of order γ^1). For the value of $\gamma = 0.005 B_0/(\text{mm})^2$ from a previous example, we get the result

$$\langle B^2 \rangle = B_0^2 + \frac{7}{45} (0.005 \frac{B_0}{(\text{mm})^2})^2 a^4.$$

For samples of $(10 \text{ mm})^2$ cross-section, the a -parameter is 5 mm, so this gives

$$\langle B^2 \rangle = B_0^2 \left[1 + \frac{7}{45} (0.005)^2 (5)^4 \right] = B_0^2 [1 + 0.0024].$$

So the experimentally-relevant value of $\langle B^2 \rangle$ is indeed bigger than B_0^2 , where B_0 is determined from the hairpin method. But it is bigger by only about +0.24% for this (example) value of γ . This is the basis for the correction suggested in Ch. 3, that

$$\langle B^2 \rangle = B_0^2 \left[1 + \left(\frac{1}{4} \pm \frac{1}{4} \right) \% \right].$$

It is interesting to note that *local* corrections to the field strength are of first order in γ , and those corrections range up to relative size $(\gamma/2) a^2 \approx 3\%$; you can show that corrections of this order occur to the magnitude of the field at the points $(x, y) = (0, \pm a)$ and $(\pm a, 0)$. Similarly, corrections to the *direction* of \mathbf{B} , also of first order in γ , occur at the corners of the square layer of sample, at $(x, y) = (\pm a, \pm a)$. But the field-value relevant to susceptibility measured by the Gouy method is not a local, but a sample-averaged, value, $\langle B^2 \rangle$, and the treatment above shows that (for a properly located sample) the corrections necessary on account of the inhomogeneity of the field are of second order in γ , and indeed negligibly small.

Validation of the inhomogeneity model

We've seen that translations-in- x of the current-hairpin, by a displacement of δ , give information on the field inhomogeneity parameter γ . But the same translation-in- x can also be carried out with a magnetic-susceptibility sample attached to the lifter structure – in fact, you might already be familiar with translating such samples in x -, y -, and z -coordinates, in each case looking for an extremum of the Δm -signal which tells you that you've located the sample properly.

But there's one more thing you can do with a translation-in- x , and that is to see how the apparent mass-change due to susceptibility depends *numerically* on the displacement δ . We expect a

quadratic dependence, showing a maximal Δm at the correct position – but given our field-inhomogeneity model, we ought now to be able to predict the *scale* of the quadratic variation. That allows the option, then, of providing a further check on the field modelling we've done in this Appendix.

The previous section shows that the vertical force F_z due to the presence (vs. the absence) of a sample creates a mass change on the balance which is proportional to $\langle B^2 \rangle$, an average taken over the area occupied by the bottom slab of the sample. We now do that very average, but over the shifted-by- δ region defined by $-a + \delta < x < a + \delta$, $-a < y < a$, and $z = 0$.

We get

$$\langle B^2 \rangle_\delta = B_0^2 + \gamma B_0 \langle y^2 - x^2 \rangle_\delta + \frac{\gamma^2}{4} \langle y^4 + 2y^2x^2 + x^4 \rangle_\delta ,$$

where the notation $\langle \rangle_\delta$ indicates the average taken over this shifted-square region.

Tedious computation of integrals gives the result

$$\langle B^2 \rangle_\delta = B_0^2 + \gamma B_0 (-\delta^2) + \frac{\gamma^2}{4} \left(\frac{28}{45} a^4 + \frac{8}{3} a^2 \delta^2 + \delta^4 \right) .$$

This can be re-arranged to give

$$\langle B^2 \rangle_\delta = [B_0^2 + \frac{7}{45} \gamma^2 a^4] + \delta^2 \left[-\gamma B_0 + \gamma^2 \left(\frac{2}{3} a^2 + \frac{1}{4} \delta^2 \right) \right] .$$

So the susceptibility signal is that arising at $\delta = 0$ (where the first bracketed term shows the previously-computed correction, of order 1/4%, to the naïve value B_0^2), plus another correction which is (as expected) quadratic in the displacement δ . Using the previous example for the size of the inhomogeneity parameter γ , we get the example result

$$\langle B^2 \rangle_\delta \cong B_0^2 \left[1 + 0.0024 - 0.005 \left(\frac{\delta}{1 \text{ mm}} \right)^2 \right] .$$

Since the Δm due to a sample's susceptibility is proportional to this $\langle B^2 \rangle_\delta$, and this Δm can be measured as a function of δ , this provides a way to look for the predicted δ -dependence, and to see if it is present with the sign and coefficient that have been predicted using the separately-measured parameter γ .

Alternatively, this result of the model can be used for reassurance. Since a sample tube can certainly be positioned *visually* to an accuracy of order 1 mm, this calculation shows that any error due to displacement-in- x is bounded by a term of size 0.005 relative to 1. That is to say, millimeter-correctness of positioning of the sample in x - (or z -)directions suffices to ensure that errors in deduced values of susceptibility χ are under 1/2%.

Appendix F: Susceptibility of anisotropic materials

Thus far we have assumed that the magnetic susceptibility of a material is a *scalar*, so that the vectors \mathbf{M} and \mathbf{H} have the same directions, and have a single proportionality constant between them, regardless of the direction of \mathbf{H} relative to the material. That's the claim of $\mathbf{M} = \chi \mathbf{H}$, which assumes that the material is 'isotropic', namely that it has the same properties along any direction. However true this might be for a gas, liquid, or powdered sample, it is *not* true for all materials. In particular, in crystalline material not belonging to the cubic classes, there is no guarantee that \mathbf{M} and \mathbf{H} will in general be parallel; and even for those special directions of \mathbf{H} that do give a parallel \mathbf{M} , there is no guarantee that the proportionality constant χ between them will have the same value along all three such 'eigen-axes'.

Here we will *not* take up the general relationship between the cause \mathbf{H} and the effect \mathbf{M} , which would require a 'susceptibility tensor' to describe it. Instead, we will take up one concrete example which is easy to investigate experimentally. Since single-crystal materials of macroscopic dimensions are generally unavailable or very expensive, we take up instead a material displaying a large magnetic anisotropy which *is* available at reasonable cost. There is the added benefit that its susceptibility (along one direction) is notably large.

That material is pyrolytic graphite, an allotrope of elemental carbon which forms on a cold substrate by deposition of atoms from a hot carbon vapor(!) in an arc furnace. Depending on the conditions, the graphite that forms can be more or less 'highly oriented', having its sheets of sp^2 -bonded carbon atoms lying in layers all parallel to the flat dimensions of a thin sample of macroscopic dimensions. (To be trendy, this is 'multi-layer graphene').

Your kit includes two pieces of this kind of graphite, in the form of sheets of size about 7.5 by 32 mm² perpendicular to the layers, and nominally $\frac{3}{4}$ mm thick. The two sheets are fit into a standard cuvette (#6 among the samples supplied) in the geometry shown here,

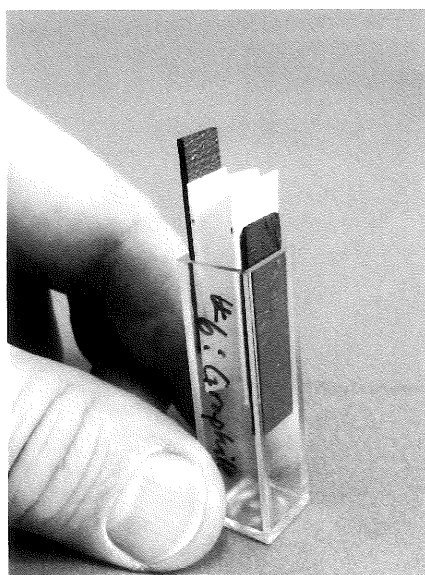


Fig. F.1: Top view of two graphite sheets, and a paper spacer, fitting into a cuvette

and this permits not only the measurement of the susceptibility of graphite by the Gouy method, but also an investigation into the anisotropy of this crystalline material.

Start by assuming the ‘book value’ of 2270 kg/m^3 for the density of graphite. Now if you measure the transverse dimensions of the sheets, and their mass, you can infer an average value for the actual thickness of the sheets that you have.

Now you can do the usual Gouy-method weighings of the cuvette, as usual positioning either the top end of the sheets, or the bottom end of the sheets, to lie in the strong-field region of your permanent magnet.

Look **first** for the dependence on orientation: which gives you the bigger apparent mass change, having the B -field perpendicular to the planes of the graphite slabs, or having the B -field parallel to these planes?

Look **next** for the sign of the mass change(s) you can see: is the magnet structure being attracted to the graphite, or repelled by it? What does this tell you about the sign of χ for graphite – is it dia- or para-magnetic?

Finally, for the orientation of B which gives you the ‘large’ Δm , what value of χ (or $\chi/\rho = \chi_{\text{mass}}$) can you deduce for your graphite? What value (or upper bound) can you assign to χ for the *other* orientation of B ?

You may find values, for the ‘good’ orientation, of $|\chi| \cong 500 \times 10^{-6}$, and $|\chi/\rho| \cong 200 \times 10^{-9} \text{ m}^3/\text{kg}$. The significance of the latter value is that its sign, and large magnitude, make graphite the easiest of all materials to *levitate* magnetically. (See Appendix G on how to demonstrate this.)

The more general point is that you have found one material exhibiting one property which you have shown to be anisotropic. You can find by reading that crystalline graphite displays *other* anisotropic properties. In particular, you’ll read that both thermal and electrical conductivity of graphite are larger for in-plane directions than for the perpendicular-to-plane direction. It is easy to make a hand-waving argument, from chemical bonds and electron clouds, explaining why this ought to be so; it is much harder to use such reasoning to compute what the magnetic susceptibility of graphite ought to be.

Appendix G: Magnetic levitation of diamagnetic materials

Every child learns that permanent magnets can attract ferromagnetic objects, and such samples can easily be lifted right off a tabletop to crash into the magnet. But stable levitation in mid-air requires either some active servo-mechanism for control, or the use of magnetic *repulsion* of a diamagnetic material. Here we work out the numerical requirements for diamagnetic levitation, to illustrate the quantitative use of measured magnetic susceptibilities.

We've seen that a volume ΔV of magnetic material in a field H experiences a vertical force

$$\Delta F_z = \frac{\mu_0}{2} \chi \frac{\partial}{\partial z} (H^2) \Delta V ,$$

and in certain circumstances this can exceed the gravitational force on the material. Consider a material of mass density ρ , so the sample mass is $\Delta m = \rho \Delta V$; the threshold condition for levitation is

$$\Delta m g = \rho \Delta V g = \frac{\mu_0}{2} \chi \frac{\partial}{\partial z} (H^2) \Delta V ,$$

so we need

$$2 \rho g = \mu_0 \chi \frac{\partial}{\partial z} (H^2) = \frac{\chi}{\mu_0} \frac{\partial}{\partial z} (B^2) .$$

This can be written as

$$2 \mu_0 g = \frac{\chi}{\rho} \frac{\partial}{\partial z} (B^2)$$

so we see that the mass susceptibility $\chi_{\text{mass}} = \chi/\rho$ is the figure of merit for a material; the higher this number, the smaller the gradient that is required to levitate the material.

For this reason, the material of choice for introductory magnetic-levitation demonstrations is HOPG or 'highly oriented pyrolytic graphite', a layered (and anisotropic) crystalline form of carbon offering a volume (mks) susceptibility of order -400×10^{-6} (for fields B in a direction perpendicular to its crystalline planes). Its density is near 2270 kg/m^3 , so it offers

$$\chi_{\text{mass}}(\text{HOPG}) \approx \frac{-400 \times 10^{-6}}{2.27 \times 10^3 \text{ kg/m}^3} = -176 \times 10^{-9} \frac{\text{m}^3}{\text{kg}} .$$

(Notice that metallic bismuth is also famously diamagnetic, but its larger density gives it a value of χ_{mass} *smaller*, ie. less favorable, than this value.)

The criterion for levitating HOPG is thus

$$\frac{\partial}{\partial z} (B^2) > \left| \frac{2 \mu_0 g}{\chi/\rho} \right| = \frac{2(4\pi \times 10^{-7} \text{ T}\cdot\text{m/A})(9.80 \text{ m/s}^2)}{176 \times 10^{-9} \text{ m}^3/\text{kg}} .$$

The payoff of using SI units is that the answer automatically emerges with the correct units,

$$\frac{\partial}{\partial z} (B^2) > 140 \frac{\text{T}^2}{\text{m}} .$$

Higher threshold values of the required gradient of field-squared can be similarly computed for other diamagnetic materials, including bismuth, antimony, and water (and, more famously, live frogs and mice – check YouTube for the video).

The lowest-cost method for achieving such large vertical gradients is to construct a two-dimensional ‘checkerboard’ array of cubes of permanent-magnet material. An infinite checkerboard of cubes laid out in the x - y plane, each of side s , creates a field \mathbf{B} in the space above the array which is periodic, in the x - and y -directions, with spatial period $\lambda = 2s$. Then Laplace’s Equation for (say) the z -component of the \mathbf{B} -field $B_z(x,y,z)$ allows for the x - (or y -) dependence of B_z such terms as

$$B_z(x) \propto \sin \text{ or } \cos(kx), \text{ with } k = \frac{2\pi}{\lambda} = \frac{\pi}{s},$$

with a similar dependence on y , provided that the z -dependence of B_z is

$$B_z(z) \propto \exp(-k\sqrt{2}z).$$

Hence in such a geometry we have $B_z^2(z) \cong \exp(-2\sqrt{2}kz)$; and if B_{\max} is the maximum field attained at the $z = 0$ surface of the array, we have approximately

$$B_z^2(z) \cong B_{\max}^2 \exp(-2\sqrt{2}kz),$$

and hence finally a vertical gradient

$$\frac{\partial}{\partial z}(B_z^2) = -2\sqrt{2}k B_{\max}^2 \exp(-2\sqrt{2}kz).$$

The gradient near the surface has a maximum value of approximately

$$\frac{\partial}{\partial z}(B^2) \cong 2\sqrt{2}k B_{\max}^2 = 2\sqrt{2}\frac{\pi}{s} B_{\max}^2.$$

Now NdFeB magnets can certainly provide surface fields of order $B_{\max} \cong 0.5$ T, and an array (even so small as a 2×2 or 3×3 checkerboard) of cubes of side $s = 1/2"$ or 12.7 mm can then potentially provide a gradient of order

$$\frac{\partial}{\partial z}(B^2) \cong \frac{2\pi\sqrt{2}}{0.0127 \text{ m}} (0.5 \text{ T})^2 = 175 \frac{\text{T}^2}{\text{m}}.$$

This is *above* the threshold for levitation of pyrolytic graphite, so it permits the sample to levitate above the $z = 0$ plane, ie. to be free-floating in the air above the magnet array. The levitation height is very small, since the necessary gradient of field-squared drops off rapidly, having a $1/e$ fall-off distance of only 1.4 mm in this example. (And the field at so low a height above the magnet array is sure to be more complicated than the simple model assumed above.)

The experimental confirmation of this prediction is quicker, easier, and certainly more definitive than the theoretical modelling above. For the proper sizes of graphite ‘floaters’, the checkerboard array also provides lateral stability in x and y ; and the stability in the z -direction is automatic. *Much* harder to predict are the equilibrium height z_0 for stable levitation, and the frequencies of small oscillations (in the x -, y -, or z -directions) about the equilibrium position;

computing any of these would require a more accurate model for the vector field B above the permanent-magnet array.

Appendix H: A case study in computing paramagnetic susceptibility

This Appendix is devoted to a theoretical calculation of a magnetic susceptibility of a ‘free-radical’ molecule, as an illustration of how such calculations are done, and how the results for the different forms (volume, mass, molar) of the susceptibility emerge. The molecule of choice is DPPH, a merciful abbreviation for the organic compound 2,2-diphenyl-1-picrylhydrazyl, whose chemical formula is $C_{18}H_{12}N_5O_6$. So it’s an organic compound, free of any transition- (or rare-earth) metal content, and you might expect it to be the usual boring diamagnetic material. But the electron count for the molecule is $6 \cdot 18 + 12 \cdot 1 + 5 \cdot 7 + 6 \cdot 8 = 108 + 12 + 35 + 48 = 203$, which is an *odd* number. (Can you think of *any* other organic molecule with an odd number of electrons?) Just how ‘odd’ this molecule is can best be seen in a chemist’s structural formula (look it up!), which reveals a nitrogen atom inside the molecule bearing only *two* (not the typical three) bonds. So DPPH is called a free radical, and given this sort of ‘dangling bond’, the surprising thing is that it’s an air-stable molecule.

Now that odd count of electrons ensures that there is an unpaired electron in each molecule of DPPH, and the structural formula shows that electron is localized to a central location inside a rather bulky molecule. So in a powder sample of bulk DPPH we have a fair approximation of a collection of solitary electron spins, one near the center of each molecule, each one available to interact with an external field, but each far enough apart in space from the next that they should interact very little with each other. We’ll assume

first, that there’s just one unpaired electron per molecule (and that we can treat it in the spin-only approximation, taking $L = 0$, so $J = S$, and $g = 2$), and

second, that this electron’s magnetic moment interacts with the external magnetic field, but not with other molecules’ moments.

(The latter is a good approximation for DPPH, even in the solid state, since the bulkiness of the molecule puts its unpaired electron far enough away from the unpaired electron of adjacent molecules. In fact, the weakness of this interaction is revealed by the fact that DPPH has to be cooled to about 0.3 K before such interactions cause the sample to become antiferromagnetic.)

Under these assumptions, we expect a molecular magnetic moment

$$\mu = g \mu_B \sqrt{J(J+1)} \rightarrow 2 \mu_B \sqrt{\frac{1}{2}(\frac{1}{2}+1)} = \mu_B \sqrt{3} ,$$

and we also expect Curie-Law behavior, with

$$\chi = \frac{\mu_0 n \mu^2}{3 k_B T} ,$$

where n is the number density of molecules.

To get that number density, note that the molar mass W , divided by Avogadro’s number N_A , gives the mass per molecule; and that molecular mass times the number density of molecules

gives $(\text{mass}/\text{molecule}) \cdot (\text{molecules}/\text{volume})$, which is $(\text{mass}/\text{volume})$ or the ordinary mass density, ρ . That is to say

$$\left(\frac{W}{N_A}\right) \cdot n = \rho, \quad \text{so} \quad n = \frac{\rho N_A}{W}.$$

Then we predict

$$\chi = \frac{\mu_0 (\rho N_A / W) (\mu_B \sqrt{3})^2}{3 k_B T} = \mu_0 \frac{\rho N_A}{W} \frac{\mu_B^2}{k_B T}.$$

Notice that the density ρ and the molar mass W both appear in this prediction; both have known values for DPPH, but their presence in this formula reveals why *other* forms of the susceptibility are more convenient than this (dimensionless, volumetric) value of χ .

For example, the more-conveniently measured mass susceptibility $\chi_{\text{mass}} = \chi/\rho$ comes out to

$$\chi_{\text{mass}} = \mu_0 \frac{N_A}{W} \frac{\mu_B^2}{k_B T},$$

which has removed the need to know the density ρ ; and the previously-defined molar susceptibility $\chi_{\text{molar}} = W \chi_{\text{mass}} = W \chi/\rho$ gives another cancellation and simplification:

$$\chi_{\text{molar}} = \frac{\mu_0 N_A \mu_B^2}{k_B T}.$$

(You could even compute the ‘molecular susceptibility’, by dividing out that factor of N_A .) So the $\chi_{\text{molar}} \cdot T$ product comes out to the ‘universal’ result

$$\chi_{\text{molar}} \cdot T = \frac{\mu_0 N_A \mu_B^2}{k_B},$$

and this ought to apply to *any* free-radical molecule matching our assumptions about one-unpaired-electron. Notice that it required electromagnetism (for the factor μ_0), quantum mechanics (providing an \hbar in μ_B), and statistical thermodynamics (for the factor k_B), all working together, to produce this prediction.

The numerical value of this result is

$$\chi_{\text{mol}} \cdot T = \frac{(4\pi \times 10^{-7} \frac{\text{T} \cdot \text{m}}{\text{A}})(6.02 \times 10^{23} \text{ /mol})(9.27 \times 10^{-24} \text{ J/T})^2}{1.38 \times 10^{-23} \text{ J/K}} = 4.71 \times 10^{-6} \frac{\text{m}^3 \cdot \text{K}}{\text{mol}},$$

so any molecule of this class has predicted room-temperature molar susceptibility of

$$\chi_{\text{mol}}(293 \text{ K}) = 16.1 \times 10^{-9} \frac{\text{m}^3}{\text{mol}}.$$

For the compound DPPH, whose molecular mass is $W = 394.32 \text{ g/mol}$, we get

$$\chi_{\text{mass}}(\text{DPPH}, 293 \text{ K}) = \frac{1}{W} \chi_{\text{mol}} = \frac{16.1 \times 10^{-9} \text{ m}^3/\text{mol}}{0.39432 \text{ kg/mol}} = 40.8 \times 10^{-9} \frac{\text{m}^3}{\text{kg}}.$$

This is not a huge susceptibility, but it is positive, and it closely matches the size of the mass susceptibility of the transition metal titanium, and is easily detected. (The calculation above omits the diamagnetism of the molecule, which will also exist and will decrease the Curie-Law susceptibility we've computed – see Appendix I.) You can *test* this prediction if you can buy (or borrow) about 3 cm³ of DPPH to fill a sample cuvette; unfortunately DPPH is not as cheap as table salt, and you might not find, even in a friendly chemistry department, anyone with this much stock of the material. (An alternative, and cheaper, air-stable free-radical material has the acronym TEMPO – check it out.)

While the positive susceptibility of DPPH sets it apart from the vast majority of organic compounds, its fame is mostly attached to its use as a calibration standard in ESR, electron spin resonance (also known as EPR, electron *paramagnetic* resonance, for reasons that should now be clear). In a non-zero static magnetic field B , the molecule's unpaired electron can be in the 'spin up' or 'spin down' state, with energy eigenvalues

$$E \left(m_s = \pm \frac{1}{2} \right) = g \left(\pm \frac{1}{2} \right) \mu_B B .$$

These two levels are separated by energy difference

$$\Delta E = g \mu_B B ,$$

and (under certain circumstances) a transition between these quantized energy levels can be driven by an oscillating magnetic field of frequency f , provided

$$h f = \Delta E = g \mu_B B , \quad \text{or} \quad f = g \left(\frac{\mu_B}{h} \right) B = g \left(\frac{e \hbar / 2m}{h} \right) B = g \frac{e}{4\pi m} B .$$

For a field of $B = 0.35$ T, this gives

$$f_{ESR} = 2 \frac{1.60 \times 10^{-19} \text{ C}}{4\pi (9.11 \times 10^{-31} \text{ kg})} (0.35 \text{ T}) = 9.78 \times 10^9 \text{ Hz} = 9.78 \text{ GHz} .$$

which conveniently falls into the 'X-band microwave' region of the spectrum. So a typical chemist's ESR spectrometer will include an electromagnet (to scan over a range of fields near 0.35 T) and an X-band microwave-waveguide system, conveying fixed-frequency microwaves into a resonant cavity containing a sample to be investigated. Since ESR is *selectively* sensitive to free-radical species, it provides a non-destructive test that's specific to even small quantities of these special molecules.

Appendix I: Diamagnetic corrections to measured susceptibilities

The previous appendix computed, under the assumption of one unpaired spin per molecule, the paramagnetic susceptibility of DPPH, or indeed any compound consistent with these assumptions. But that result omits the effects of the *rest* of the molecule, assumed to be composed of paired electrons giving only a diamagnetic effect. Proper comparison of a measured value for susceptibility of DPPH with the theory of Curie paramagnetism would require a correction for the diamagnetism that is present in the actual molecules, but absent in the Curie-Law calculation.

Such corrections can indeed be made, and they form a sort of ‘background’ in the sub-discipline of magnetochemistry. We care about those corrections here, because they are a part of a full theoretical prediction of the susceptibility of a molecular sample. In particular, their neglect would be to assume that the observed susceptibility (say, for a paramagnetic sample) ought to follow the Curie Law, whereas in fact, it’s only the *paramagnetic part* of the susceptibility that ought to follow the Curie Law.

Now the diamagnetism of a molecule can in principle be calculated directly from the electronic wavefunction of the molecule, as illustrated by the computation in Ch. 2 of helium’s diamagnetic susceptibility directly from the Schrödinger Equation. But a first-principles quantum-mechanical calculation of the wavefunction of a complicated molecule is a computationally-prohibitive task, and plenty of approximations have to be made to make it at all feasible. Given the empirical nature of some of these assumptions, it turns out in practice that the first-principles computation of susceptibility can sometimes be *replaced* by estimates derived from experimental data on simple molecules, combined with the empirical observation that the susceptibility of a molecule is (close to) the sum of the susceptibilities of its constituent parts.

Here is an example of some empirical evidence that the diamagnetic susceptibility of molecules can in fact be estimated by this sort of summation. This example comes from an organic chemist’s favorite series of molecules, the alkane series of hydrocarbons methane, ethane, propane, butane . . . octane, nonane, etc. These have the chemical formulae C_nH_{2n+2} , and (in their simplest molecular forms) have the linear, or chain, structure $H(CH_2)_nH$, with $n=1$ meaning methane, $n=2$ ethane, $n=8$ octane, and so on. Each of these hydrocarbons has had its magnetic susceptibility measured; all of them are diamagnetic, and the results look very different depending on whether we list the (volume) susceptibility or the molar susceptibility. Giving the results in the historic language of magnetochemistry, we get the cgs forms of susceptibility from handbook references, here supplying the correct units (as such references so rarely do):

Alkane name	n -value	$\chi^{(cgs)}$	$\chi^{(cgs)}_{\text{molar}}$
Methane	1	-0.765×10^{-6}	$-12.27 \times 10^{-6} \text{ cm}^3/\text{mole}$
Ethane	2	-0.910×10^{-6}	$-27.37 \times 10^{-6} \text{ cm}^3/\text{mole}$
Propane	3	-0.919×10^{-6}	$-40.5 \times 10^{-6} \text{ cm}^3/\text{mole}$
Butane	4	-0.988×10^{-6}	$-57.4 \times 10^{-6} \text{ cm}^3/\text{mole}$
Pentane	5	-0.874×10^{-6}	$-63.05 \times 10^{-6} \text{ cm}^3/\text{mole}$

Hexane	6	-0.865×10^{-6}	$-74.6 \times 10^{-6} \text{ cm}^3/\text{mole}$
Heptane	7	-0.851×10^{-6}	$-85.24 \times 10^{-6} \text{ cm}^3/\text{mole}$
Octane	8	-0.846×10^{-6}	$-96.63 \times 10^{-6} \text{ cm}^3/\text{mole}$
Nonane	9	-0.843×10^{-6}	$-108.13 \times 10^{-6} \text{ cm}^3/\text{mole}$

The table could be extended, but it already shows two things: the ordinary (or volumetric) susceptibility shows numerical values comparable to that for water, with a very *uninformative* variation with n , but the molar susceptibility displays a striking linear variation with n . In fact the molar susceptibility can be fit (try it out!) to

$$\chi_{molar}^{(cgs)}(n) = (-4.80 - 11.56 \cdot n) \times 10^{-6} \text{ cm}^3/\text{mole} .$$

This suggests that a mole of CH₂ groups contributes (for purposes of diamagnetic susceptibility) a volume of $11.56 \times 10^{-6} \text{ cm}^3$, while the mole of fixed (H- and -H) end units of the chain contribute a volume of $4.80 \times 10^{-6} \text{ cm}^3$. [The $n=0$ member of this series is H-H, or just the H₂ molecule – what does the linear relation predict for *its* susceptibility? And how does this compare to the *measured* (molar) susceptibility of molecular hydrogen?] So the lesson of this variation is that as the length of the chain grows, its ‘diamagnetic volume’ grows. So, of course, does the actual molecular volume, creating trends in mass density (not shown), and in volumetric susceptibility, that are complicated and uninteresting, but also giving a trend in *molar* susceptibility that is predictive and useful.

This discovery has been extended from this case of -CH₂- groups to many more chemical modules, yielding a set of empirical rules that magnetochemists use to predict the (diamagnetic part of the) molar magnetic susceptibility for quite general compounds, in the form

$$\chi_{molar}^{(cgs)} = \sum_i \chi_i + \lambda ,$$

where the sum is over all atoms (or groups) in a molecule, and where the constant λ is due to structural features not captured in mere atom count. The χ_i attributable to individual atomic constituents or groups are called “Pascal’s constants”, and they are listed in various references; see in particular Bain & Berry, J. Chem. Ed. 85, 532 (2008).

The use of this method outside the fraternity of magnetochemists requires two kinds of experience: first there is the atom- and group-counting required, plus the structural complications modeled in λ ; but next there is the conversion into ‘real units’. We take up that effort in two stages, illustrated by examples.

The (diamagnetic contribution to the) susceptibility of Mohr’s salt

Mohr’s salt is a convenient and stable compound containing iron in its ferrous, Fe(II) or Fe²⁺ form, and it is paramagnetic because of its transition-metal content. But if that paramagnetism could magically be ‘turned off’, there would still remain the diamagnetism of the molecule, (NH₄)₂Fe(SO₄)₂·6H₂O . Here’s how that would be estimated. We imagine one mole of the

(solid, crystalline) compound, and we find, in various references, the ‘Pascal’s constants’ of -13 for each H₂O molecule, -13 for each NH₄⁺ ion, -13 for the (diamagnetic behavior of the) Fe²⁺ ion, and -40 for each SO₄²⁻ ion. (Clearly, there’s a long history of comparative empirical measurements that lie behind these values for the constants!) But for our whole molecule, we just add up to get the net prediction

$$(2 \times -13) + (1 \times -13) + (2 \times -40) + (6 \times -13) = -197,$$

and we understand the latter to mean a diamagnetic contribution to $\chi^{(\text{cgs})}$ _{molar} (Mohr’s salt) of $-197 \times 10^{-6} \text{ cm}^3/\text{mole}$. We convert that into its mks form below, after doing another example.

The (diamagnetic contribution to the) susceptibility of TEMPO

TEMPO, or 2,2,6,6-Tetramethylpiperidin-1-yl)oxyl, C₉H₁₈NO, is a rather exotic free-radical organic molecule, one having a solitary oxygen atom hanging, by only a single bond, onto a nitrogen atom that’s part of a six-membered ring. (Look up its chemical structure.) Unlike some other compounds with this sort of N-O* character, TEMPO is air-stable, and it also doesn’t dimerize into a diamagnetic material in its solid form. The interest in TEMPO comes from its *odd* number of electrons, which makes it paramagnetic. To work out the background *diamagnetism* of the molecule, we work first on its four methyl (-CH₃) groups; we look up Pascal constants -6.0 for a carbon, and -2.9 for a hydrogen, and so estimate -14.7 for a methyl group. We also look up -6.0 for each (of five) carbons in that ring, -4.6 for a nitrogen, and -4.6 for an oxygen, and note there are no structure contributions (no benzene ring, no C=C double bond, etc.) So we then estimate a total of

$$(4 \times -14.7) + (5 \times -6.0) + (1 \times -4.6) + (1 \times -4.6) = -98.0,$$

and we understand the latter to mean a diamagnetic contribution to $\chi^{(\text{cgs})}$ _{molar} (TEMPO) of $-98.0 \times 10^{-6} \text{ cm}^3/\text{mole}$.

Converting to mks molar susceptibilities

These contributions are computed within the cgs recipe for susceptibilities, so to be converted to mks susceptibilities, they have to be multiplied by 4π . Then we can also use $1 \text{ cm}^3 = 10^{-6} \text{ m}^3$ to write our estimates as

$$\chi^{(\text{mks})}\text{molar} \text{ (Mohr's salt)} = 4\pi \times -197 \times 10^{-6} (10^{-6} \text{ m}^3)/\text{mole} = -2.48 \times 10^{-9} \text{ m}^3/\text{mole},$$

$$\text{and } \chi^{(\text{mks})}\text{molar} \text{ (TEMPO)} = 4\pi \times -98.0 \times 10^{-6} (10^{-6} \text{ m}^3)/\text{mole} = -1.23 \times 10^{-9} \text{ m}^3/\text{mole}.$$

These are still *molar* susceptibilities, the only form suited for the Pascal-constant additivity we have done. But since molar susceptibility is also the level at which we typically compare theory and experiment, we would thus predict, for TEMPO at 293 K, a net (paramagnetic + diamagnetic) molar susceptibility of

$$\chi_{\text{molar}}(\text{TEMPO}) = (+16.1 \times 10^{-9} \text{ m}^3/\text{mole}) + (-1.2 \times 10^{-9} \text{ m}^3/\text{mole}) = 14.9 \times 10^{-9} \text{ m}^3/\text{mole}.$$

Here the first term is the paramagnetic contribution, computed as in Appendix H. Thus we see a fairly large (-8%) diamagnetic correction for the not-strongly-paramagnetic free-radical material TEMPO. By contrast, you can show that for Mohr's salt, the diamagnetic correction is a rather smaller part of the net predicted susceptibility. Alternatively, you can measure (using the Gouy method) the *mass* susceptibility of Mohr's salt; you can convert that to a measured value of the *molar* susceptibility; and then writing

$$\chi_{\text{molar}}(\text{Mohr's salt}) = \chi_{\text{molar}}^{(\text{para})}(\text{Mohr's salt}) + \chi_{\text{molar}}^{(\text{dia})}(\text{Mohr's salt})$$

you can correct the experimentally-measured value to the paramagnetic part alone,

$$\begin{aligned}\chi_{\text{molar}}^{(\text{para})}(\text{Mohr's salt}) &= \chi_{\text{molar}}(\text{Mohr's salt}) - \chi_{\text{molar}}^{(\text{dia})}(\text{Mohr's salt}) \\ &= \chi_{\text{molar}}(\text{Mohr's salt}) - (-2.5 \times 10^{-9} \text{ m}^3/\text{mole}) .\end{aligned}$$

The right-hand-side of this equation combines an experimental measurement of the total susceptibility and an empirical estimate for the diamagnetic part of it, so the left-hand-side then gives the purely-paramagnetic part of the molecule's susceptibility. And this, finally, is the result that ought to be compared to a Curie-Law theory.

Appendix J: The internal field in diamagnetic water

The Gouy method you've used, in its TeachSpin realization, is sensitive enough to detect the diamagnetism of water. This Appendix takes up the implications of that diamagnetism for the 'internal field' inside a bulk sample of water, and illustrates thereby the difference between the volume-averaged, and the local, values of the magnetic field inside matter.

We start with the book-value (corrected-to-mks) volume susceptibility of water at 293 K, of

$$\chi(\text{water, 293 K}) = -9.05 \times 10^{-6} .$$

Then we recall the fundamental definitions $B = \mu_0 (H + M)$ and $M = \chi H$ to derive

$$B = \mu_0 (H + M) = \mu_0 (H + \chi H) = \mu_0 H(1 + \chi) .$$

This shows that inside a diamagnetic sample (where $\chi < 0$), the B -field is *smaller* in magnitude than it would be in the absence of the sample, ie. in vacuum. So we imagine a small spherical sample of water immersed into a previously-uniform field B in space: because the sample is (dia)magnetic, the field lines of B are distorted, and are partly 'ejected' from inside the sample, leaving B smaller inside.

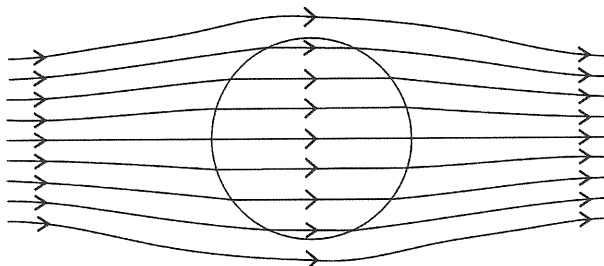


Fig. J.1: a sketch of magnetic field lines interacting with a (rather strongly!) diamagnetic sphere

(We pick the sample to be *spherical* just to ensure that the B -field's magnitude is spatially uniform -- though of reduced value -- over the full volume of the sphere.) The limiting case of this process is the Meissner effect in Type-I superconductors, which *fully eject* the field B from their interior; this can be described by assigning an (mks) susceptibility of -1.0 to such materials.

So immersed in a B -field that is asymptotically uniform and of strength B_{out} , a sphere of water defines a region in which the field is also uniform, but of smaller value:

$$B_{\text{in}} = B_{\text{out}}(1 + \chi) = B_{\text{out}}(1 - 9.05 \times 10^{-6}) = B_{\text{out}}(0.999\,990\,95) .$$

This tiny departure from a factor-of-one provides a measure of how very weak an effect is the diamagnetism of water.

But is there any independent test of this claim that the field inside water is some parts-per-million (ppm) smaller than the asymptotic field outside? Indeed there is, and it comes from doing proton NMR (nuclear magnetic resonance) on the nuclei of the hydrogen atoms in the water molecule.

NMR depends on protons (of spin $1/2$) having two allowed spin states in a magnetic field B , and taking on two distinct energy levels in such a field:

$$E \rightarrow E_{\pm} = (-\mu \cdot B)_{\pm} = -\gamma_p I_{\pm} \cdot B = -\gamma_p \left(\pm \frac{\hbar}{2} \right) B_z .$$

Here we've introduced γ_p as the gyromagnetic ratio of a proton, which connects its magnetic moment μ with its spin angular momentum I ; and we've taken the field direction to define the z -axis, along which direction I has only the two allowed projections of $\pm \hbar/2$. There is an energy difference ΔE between these two spin states, and this energy difference can be 'bridged' by a quantum transition at angular frequency ω , provided that we observe the Bohr condition

$$\hbar \omega = \Delta E = \gamma_p \hbar B_z .$$

So the (ordinary) frequency f that can be detected in an NMR experiment is

$$f = \frac{\omega}{2\pi} = \left(\frac{\gamma_p}{2\pi} \right) B_z .$$

You can look up the gyromagnetic ratio γ_p for protons, for example in the NIST table of fundamental constants at <http://physics.nist.gov/cuu/Constants/>, and you will find *two* values quoted:

$$\frac{\gamma_p}{2\pi} = 42.577\,4806\,(10) \text{ MHz/T} ;$$

$$\frac{\gamma_p'}{2\pi} = 42.576\,3866\,(10) \text{ MHz/T} .$$

The numbers both show, in parentheses, the uncertainty in the final digits of their values. The two numbers *differ*, because they apply to two distinct situations: the first applies to bare protons in a magnetic field, and the second applies to protons inside water molecules in a spherical sample of water at 25 °C in a magnetic field. So compared to a bare proton, a proton in water acts (for NMR purposes) as if it's immersed in a field that is smaller than the external field, by the factor

$$42.576\,3866 / 42.577\,4806 = 0.999\,974\,31 = 1 - 25.7 \times 10^{-6} .$$

So for a magnetic field that's uniform asymptotically, and a sphere of water in that field, we have *two* measures for the internal field:

- The volume-averaged field inside the sphere is weaker, by 9.05 ppm, than the asymptotic field.
- The *local* field, at the sites of the protons in hydrogen atoms in the water molecules, is weaker, by 25.7 ppm, than the asymptotic field.

Both of these illustrate the diamagnetic effects of water, but they also illustrate the difference between a field averaged over the whole volume of water (including space within, and between, molecules) and the field's 'local' value (appropriate to the location of a proton). Yet another local field value could be measured (using ^{17}O NMR), one that's appropriate to the location of the nuclei of *oxygen* atoms in molecules of water. Because these local values differ from the

volume-averaged value, NMR can be used to measure the difference in the field at (say) distinct proton sites inside a molecule, which is one of the reasons that proton NMR is so supremely useful to a chemist. A chemist speaks of the ‘shielding’ effect of the molecular environment, in decreasing the magnetic field from its asymptotic value to its local value. The *variation* of this shielding effect at various locations within the molecule explains why the NMR spectrum of ethanol, $\text{CH}_3\text{CH}_2\text{OH}$, shows signals at three slightly different frequencies, due to the three distinct environments in which protons are found in this molecule.

Appendix K: Some project ideas for Foundational Magnetic Susceptibility

This Appendix describes more things you can do with your Foundational Magnetic Susceptibility apparatus, and with your newly-acquired competence in dealing with measurement and modelling of magnetic properties.

Of course you can measure the 16 samples supplied with the TeachSpin apparatus. Each one has been picked for a reason; the solid samples will require a different data-reduction strategy than the powdered samples. Two of the samples are ferromagnetic, so a constant- χ model is probably inappropriate to them, but they've been included to show how *large* a nominal value of χ emerges from a measurement.

Next, you have a large collection of empty cuvettes, each available for filling with a sample of your choice. We suggest that students use familiar materials and measure them, starting with water, salt, sugar, baking soda, and the like, and graduating to less edible and more interesting materials. Once students learn that paramagnetism is a special phenomenon, they can focus their search for new materials toward the more promising classes of substances with transition-metal or rare-earth content. Or, they can try ‘magnetic surveying’, starting with geological samples (what about beach sand?), or even try ‘magnetic refining’ or ‘magnetic concentration’ of original raw samples. What can magnetism teach one about Portland cement (concrete mix), for example?

It would be a valuable exercise for a student to show that a soluble material in crystalline form, and the same material in water solution, can give the same result for the *molar* susceptibility. That is to say, students can show that paramagnetism is a property belonging to each ion (and not a cooperative phenomenon like ferromagnetism). Once students learn about measurements in solution, they could try dilution – does the raw magnetic signal seen on the balance *scale* properly with the concentration of the relevant ion? How dilute a solution can still be detected by its paramagnetism?

Students can also check to see that ionic magnetism really does depend on chemical valency. It is feasible to use cuprous and cupric oxide, Cu₂O and CuO, as a pair of samples. Cuprous oxide is semi-stable in air (though it does convert, slowly, to cupric oxide upon exposure to moist air). Lemonade could be made of this lemon by having the students execute the conversion deliberately, and seeing if the susceptibility changes accordingly.

Another valency investigation can be performed using Fe(II), ferrous vs. Fe(III), ferric salts of iron.

A famous textbook illustration in paramagnetism can be re-created with the acquisition of a *series* of samples, taking one right across the transition metals (scandium through zinc) or right across the rare earths (yttrium through lutetium). It is not necessary to get metallic samples – chlorides or nitrates would work just as well. Nor is it required to plot results as a function of

atomic number Z – more revealing is to plot as a function of net electron number of the *ion* in the compound chosen. (Example: gadolinium has $Z=64$, but the Gd^{3+} found in the oxide Gd_2O_3 has electron count 61.) Students will find that while for transition metals the spin-only approximation gives theoretical results matching the data, the case of rare-earth metals is different, and more elaborate theory is needed.

[With the right sort of equipment, a set of rare-earth samples of this sort can also be used, equally non-destructively, as part of a systematic investigation of X-ray fluorescence as a function of atomic number, aimed at testing Moseley's Law. The procurement of such samples will even reveal, via the market prices(!) of elemental samples, a consequence of their relative terrestrial abundance, which is itself an outcome of stellar nucleosynthesis captured in the Oddo-Harkins Rule.]

One historically-famous feature of the Curie Law for paramagnetism is its predicted dependence on the (absolute) temperature of the sample. The TeachSpin Foundational Magnetic Susceptibility apparatus is not really suited to a systematic investigation of this dependence, but *indications* of the presence of the effect can still be found. A cuvette and its contents can quite easily be chilled in a freezer, or heated in a warm-air bath, to bring its contents eventually to (say) -10°C or $+50^\circ\text{C}$. (The polystyrene plastic of the cuvettes will soften above 80°C .) It is not so easy to *preserve* these temperatures for long enough to measure the samples using the Guoy technique – though a handmade sleeve of thin Styrofoam material could be used to insulate the sample, even while it's inside the magnet for measurement. Neither is there a really good way to measure the actual temperature of the sample as it reverts toward room temperature. But it could still be worthwhile to make the attempt, just to show if changes can be seen, of the approximate ($\pm 10\%$) size, and sense, predicted by the Curie Law.

A fine comparison of Curie theory and experiment can be achieved by measuring the (room-temperature) magnetic susceptibility of (powdered samples of) free-radical material. Appendix H discusses the case of the EPR-famous free-radical material DPPH, but another free-radical material, (2,2,6,6-tetramethylpiperidin-1-yl)oxidanyl or TEMPO, is perhaps a better choice for price and availability. Either material presents one unpaired electron per molecule, and allows a first-principles calculation of the expected paramagnetic susceptibility.

Another class of projects is open to students with actual chemistry experience, or to interdisciplinary teams with chemistry-student participation. Here are some ideas worthy of investigation:

There are transition-metal compounds that exhibit ‘high spin’ and ‘low spin’ behavior. Sticking just to iron complexes of octahedral geometry, a soluble ferrous salt, $\text{Fe}(\text{II})$, will dissolve in water to form the complex $[\text{Fe}(\text{H}_2\text{O})_6]^{2+}$, and its molar susceptibility can be measured, and converted to give the effective value of μ/μ_B for the $\text{Fe}(\text{II})$ ion. For comparison, there is the $\text{Fe}(\text{II})$ coordination compound potassium ferrocyanide trihydrate, $\text{K}_4[\text{Fe}(\text{CN})_6] \cdot 3\text{H}_2\text{O}$, which contains the same Fe^{2+} ion, complexed under the same octahedral geometry. Its susceptibility can be measured for the dry compound, no water-solution required; what value of μ/μ_B does it give?

The same comparison can be made with Fe(III) or ferric compounds. Dissolving ferric chloride in water will give the complex $[\text{Fe}(\text{H}_2\text{O})_6]^{3+}$, whose molar susceptibility can be measured, and converted to give the effective value of μ/μ_B for the Fe(III) ion. For comparison, there is the Fe(III) coordination compound potassium ferricyanide, $\text{K}_3[\text{Fe}(\text{CN})_6]$, which contains the same Fe^{3+} ion, complexed under the same octahedral geometry. Its susceptibility can also be measured for the dry compound; what value of μ/μ_B does it give?

{Note that ferric chloride forms a somewhat corrosive solution. Note also that despite their baleful names, ferrocyanides and ferricyanides are perfectly safe to handle, so long as they're kept away from strong acids. As always, *read* about chemical compounds before using them.}

There are a host of other transition-metal complexes that can be made with relatively simple chemical reactions. One famous starting point is the hexaammine copper(II) complex that can be made from aqueous copper sulfate and ammonia. Quite apart from producing some remarkably colorful materials, complexes such as these leave ions in states of bonding that permit predictions of expected magnetic properties. In other words, certain hypotheses for chemical bonding for such complexes can be *falsified* by magnetic measurements. And very complicated complexes can nowadays be made, using artfully chosen reagents – an inorganic chemistry textbook will discuss these topics under the title ‘coordination chemistry’. A host of complexes involving nickel and cobalt are known, but ones with manganese or chromium content are just as worthy of making and measuring.

There are also complexes of immense biological interest, typified by chlorophyll and hemoglobin. Students ought to see, and ponder, the chemical structure of these two molecules, and to see the role that magnesium and iron (respectively) play in them. If they can get enough sample material of each, they can test the one for diamagnetism, and the other for paramagnetism. There is also a relatively simple process that will turn chlorophyll into ‘chlorophyllin’, and a search for the sodium-copper chlorophyllin complex known as ‘natural green 3’ (aka. E141) will reveal a material, derived from (diamagnetic) chlorophyll, that ought to be paramagnetic.

Can magnetic susceptibility be changed by a chemical reaction, *in situ*? How does the magnetic susceptibility of two-component epoxy adhesive change, during its slow curing process? Can you find a reaction of a free-radical species with something else, preferably one slow enough to ‘follow’ via magnetic susceptibility? Better still, is there such a reaction which you can *monitor* happening in real time, via a color change? How about treating a solution of ferrous iron with hydrogen peroxide? You might look into this topic under the keywords “magnetic titration”.

Can magnetic susceptibility of a solution be changed by an electro-chemical process, *in situ*? Could a cuvette be fitted with electrodes to allow electrolysis, and make this happen in real time?

Could magnetic susceptibility be detected in the biochemically interesting case of iron-sulfur proteins? Look up ferredoxin, and read about the $\text{Fe}(\text{II}) \cdot \text{Fe}(\text{III}) \leftrightarrow \text{Fe}(\text{III}) \cdot \text{Fe}(\text{III})$ reaction at the core of a protein molecule which gives this protein a role in oxidation-reduction processes.

Could you synthesize nanoscale iron-oxide based particles too small to exhibit ferromagnetism, yet still display ‘superparamagnetism’ in their properties?

Appendix L: What is a Bohr magneton?

This Appendix describes the concept of the ‘magneton’, and illustrates the motivation for the ‘Bohr magneton’ μ_B , a standard unit for magnetic moment.

Classical and Quantum orbital magnetic moments

Recall that magnetic moment μ is a vector associated with a magnetic system. It gives the system’s response to immersion in an external B -field, either as torque

$$\tau = \mu \times B ,$$

or as an energy of interaction,

$$E = -\mu \cdot B .$$

Recall also that a planar loop of current i , whose circumference spans an area A , has a magnetic moment of size

$$\mu = i A .$$

From these facts we can compute the magnetic moment expected for a system in which a particle of charge q makes a classical circular orbit of radius r and speed v . The ‘time per orbit’ T is then (circumference)/(speed), so $T = (2\pi r)/v$, and the effective current is charge-per-unit-time,

$$i = \frac{q}{T} = \frac{q}{2\pi r/v} = \frac{q v}{2\pi r} .$$

Then the magnetic moment of this circulating charge is

$$\mu = i A = \left(\frac{q v}{2\pi r} \right) (\pi r^2) = \frac{q v r}{2} .$$

If the particle involved has mass m , then the quantity $|r \times p| = mvr$ gives the angular momentum L of the orbiting particle. So we can write

$$\mu = \frac{q v r}{2} = \frac{q}{m} \cdot \frac{m v r}{2} = \frac{q}{2m} \cdot L ,$$

and this result shows that the magnetic moment μ is expected to be proportional to the angular momentum L . We have also predicted classically that the constant of proportionality, in general called the gyromagnetic ratio γ , has the value $\gamma = q/(2m)$.

Now if that relationship remains true in quantum mechanics, and if angular momentum is quantized in quantum mechanics, then it follows that magnetic moment is expected to be quantized as well. That suggests that we should find, experimentally, systems with not just any values of magnetic moment, but instead values falling onto a list of discrete values.

An early empirical search for such quantization popularized the ‘Weiss magneton’ as a unit in which magnetic moments might be quantized; clearly, this was a parallel to the fundamental charge e as the unit in which all charges were quantized. And this came in an era of discovery in which internal energies of atomic systems were found to be quantized, as well. But the magneton we know today comes from a better-developed line of theoretical thought, arising from Bohr models of atomic orbits. For a Bohr treatment of our example of orbital motion, we expect the angular momentum L to be quantized in integer multiples of Planck’s constant, so we expect $L \rightarrow L_n = n \hbar$, suggesting that magnetic moments ought to obey

$$\mu \rightarrow \mu_n = \gamma \cdot L_n$$

where n is an integer ($0, 1, 2, \dots$), so that magnetic moments ought to have values

$$\mu_{\text{orbital}} = \left(\frac{q}{2m}\right)(L_n) = \frac{q}{2m} \cdot n\hbar .$$

For the case of an electron as orbiting particle, we have $q = -e$, so we’d expect

$$\mu \rightarrow \mu_n = n \frac{e\hbar}{2m_e} ,$$

where m_e emphasizes that we’re specializing to the electron’s mass. The combination that has emerged,

$$\mu_B \equiv \frac{e\hbar}{2m_e} ,$$

is called the Bohr magneton. It arises naturally in connection with Bohr-orbital models, and it generates a prediction of ‘the magneton’, the unit in terms of which all (electronic) magnetic moments are expected to be quantized.

Spin, and associated magnetic moments

The discussion thus far leaves out completely the highly relevant case of *spin* or intrinsic angular momentum, and thus also leaves out any magnetic moments associated with that new kind of angular momentum. For electrons, spin angular momentum is not an integer $\times \hbar$, but has the single value $\hbar/2$ instead. But there is also the countervailing fact that the gyromagnetic ratio for spin is not the classically-expected $\gamma = q/(2m)$, but is bigger by a dimensionless ‘g-factor’, whose value is predicted to be 2 (in Dirac theory), or is corrected to 2.0032... (in quantum electrodynamics). So for spin angular momentum S , we expect magnetic moment

$$\mu_{\text{spin}} = \gamma_{\text{spin}} S = \left(g \frac{q}{2m}\right) \left(\frac{\hbar}{2}\right) ,$$

so that for an electron, we expect

$$\mu_{\text{spin}} = \left(\frac{g}{2}\right) \cdot \frac{e\hbar}{2m_e} \cong \frac{e\hbar}{2m_e} = \mu_B .$$

Thus it turns out that for electrons in *either* orbital or spin cases, the natural unit of quantized magnetic moment remains the Bohr magneton μ_B . Its numerical value is about

$$\mu_B = \frac{(1.602 \times 10^{-19} \text{ C})(1.055 \times 10^{-34} \text{ J}\cdot\text{s})}{2(9.109 \times 10^{-31} \text{ kg})} \cong 9.274 \times 10^{-24} \text{ J/T.}$$

The theoretical development of Curie paramagnetism in Ch. 2 shows that the full application of modern quantum mechanics does not support mere integer-multiple quantization of magnetic moments, $\mu = n \mu_B$, but instead predicts more complicated (yet still quantized) behavior, $\mu \rightarrow \mu_{\text{eff}} = g_J \mu_B [J(J+1)]^{1/2}$. Yet even so, the Bohr magneton remains the natural unit in which magnetic moments of *any* electron-based origin are naturally reported, such that the dimensionless ratio μ/μ_B is the natural way in which results might best be quoted, even for a purely empirical measurement. [If you've dealt with cgs units for reported quantities, you'll have a fresh appreciation for a dimensionless ratio, such as $\mu/\mu_B = 1.73$. In particular, in this form of giving a result, you need not quote, or even know, the units of μ (and μ_B) at all.]